Kaplan, J. I., & Fraenkel, G. (1980) *NMR of Chemically Exchanging Systems*, pp 74-80, Academic Press, New York.
Kearns, D. R., & Shulman, R. G. (1974) *Acc. Chem. Res. 7*, 33-39.
Khorana, H. G. (1968) *Pure Appl. Chem. 17*, 349-381.
Lee, C. H., & Tinoco, I., Jr. (1980) *Biophys. Chem. 11*, 283-294.
Lee, C. H., Ezra, F. S., Kondo, N. S., Sarma, R. H., & Danyluk, S. S. (1976) *Biochemistry 15*, 3627-3638.
Martin, F. H., & Tinoco, I., Jr. (1980) *Nucleic Acids Res. 8*, 2295-2299.
Martin, F. H., Uhlenbeck, O. C., & Doty, P. (1971) *J. Mol. Biol. 57*, 201-215.
Milman, G., Langridge, R., & Chamberlin, M. J. (1967) *Proc. Natl. Acad. Sci. U.S.A. 57*, 1804-1810.
Pardi, A. (1980) Ph.D. Thesis, University of California, Berkeley.
Patel, D. J. (1974) *Biochemistry 13*, 2396-2402.
Patel. D. J. (1975) *Biochemistry 14*, 3984-3989.
Patel, D. J. (1979) *Eur. J. Biochem. 96*, 267-276.
Patel, D. J., & Hilbers, C. W. (1975) *Biochemistry 14*, 2651-2656.
Porschke, D., & Eigen, M. (1971) *J. Mol. Biol. 62*, 361-381.
Ravetch, J., Gralla, J., & Crothers, D. M. (1973) *Nucleic Acids Res. 1*, 109-127.
Redfield, A. G., Kunz, S. D., & Ralph, E. K (1975) *J. Magn. Reson. 19*, 114-117.
Robillard, G. T., & Reid, B. R. (1979) in *Biological Applications of Magnetic Resonance* (Shulman, R. G., Ed.) pp 45-112, Academic Press, New York.
Sarma, R. H. (1980) *Nucleic Acid and Geometry and Dynamics*, Pergamon Press, New York.
Selsing, E., Wells, R. D., Early, T. A., & Kearns, D. R. (1978) *Nature (London) 21*, 249-250.
Shum, B. W. K. (1977) Ph.D. Thesis, Yale University.
Ts'o, P. O. P., Kondo, N. S., Schweizer, M. P., & Hollis, D. P. (1969) *Biochemistry 8*, 997-1029.
Ts'o, P. O. P., Barrett, J. C., Kan, L. S., & Miller, P. S. (1973) *Ann. N.Y. Acad. Sci. 222*, 290-306.
Uhlenbeck, O. C., Martin, F. H., & Doty, P. (1971) *J. Mol. Biol. 57*, 217-229.
Warshaw, M. M. (1965) Ph.D. Thesis, University of California, Berkeley.
Washaw, M. M., & Tinoco, I., Jr. (1966) *J. Mol. Biol. 20*, 29-38.
Warshaw, M. M., & Cantor, C. R. (1970) *Biopolymers 9*, 1079-1103.

Study of Transfer Ribonucleic Acid Unfolding by Dynamic Nuclear Magnetic Resonance†

Paul D. Johnston‡ and Alfred G. Redfield*

ABSTRACT: Nuclear magnetic resonance (NMR) measurements of proton exchange were performed on yeast $tRNA^{Phe}$, and in much less detail on *Escherichia coli* $tRNA^{fMet}$, over a range of Mg^{2+} concentrations and temperatures, at neutral pH and 0.1 M NaCl. The resonances studied were those of ring nitrogen protons, resonating between 10 and 15 ppm downfield from sodium 3-(trimethylsilyl)-1-propanesulfonate, which partake in hydrogen bonding between bases of secondary and tertiary pairs. Methods include saturation-recovery, line width, and real-time observation after a change to deuterated solvent. The relevant theory is briefly reviewed. We believe that most of the higher temperature rates reflect major unfolding of the molecule. For *E. coli* $tRNA^{fMet}$, the temperature dependence of the rate for the U8-A14 resonance maps well onto previous optical T-jump studies for a transition assigned to tertiary melting. For yeast $tRNA^{Phe}$, exchange rates of several resolved protons could be studied from 30 to 45 °C in zero Mg^{2+} concentration and had activation energies on the order of 40 kcal/mol. Initially, the tertiary structure melts, followed shortly by the acceptor stem. At high Mg^{2+} concentration, relatively few exchange rates are measurable below the general cooperative melt at about 60 °C; these are attributed to tertiary changes. Real-time observations suggest a change in the exchange mechanism at room temperature with a lower activation energy. The results are compared with those obtained by other methods directed toward assaying ribonucleic acid dynamics.

Knowledge of the modes of flexibility of transfer ribonucleic acid (tRNA) is interesting in itself and is relevant to other RNA classes. The rates of exchange with solvent of labile protons within tRNA are likely to reflect such flexibility. Nuclear magnetic resonance (NMR) provides a potentially powerful way to study exchange rates, provided that resonances can be identified. The present paper summarizes our measurements of such rates as a function of temperature and magnesium concentration, and their interpretation in light of recent studies directed toward identification (Johnston & Redfield, 1981).

Physical studies of tRNA have been reviewed by Crothers & Cole (1978) and Crothers (1979). There is good evidence that in the presence of 0.1 M NaCl, as used in our work, the structure of tRNA approximates the native, active form whether magnesium is present or not. In the presence of magnesium, the native structure is stable to fairly high tem-

† From the Department of Biochemistry, Brandeis University, Waltham, Massachusetts 02254. *Received January 12, 1981.* This work was supported in part by U.S. Public Health Service Grants GM20168 and 5T01-GM0212 and by the Research Corporation. This is Publication No. 1368 of the Brandeis University Biochemistry Department. A.G.R. is also at the Physics Department and the Rosensteil Basic Medical Sciences Research Center of Brandeis University.

‡ Present address: Institute of Molecular Biology, University of Oregon, Eugene, OR 97403.

0006-2960/81/0420-3996$01.25/0

peratures (~60 °C) and melts almost entirely in one step, whereas in zero magnesium concentration, melting starts at a lower temperature and appears to occur as a sequence of several steps (Privalov & Filimonov, 1978). It is generally assumed that the tertiary structure melts first, followed by independent melting of the four secondary helixes (Stein & Crothers, 1976).

X-ray diffraction studies indicate several magnesium binding sites, but do not indicate their strength. Binding studies show the expected 20–25 loosely bound Mg^{2+} ions and a few tightly bound ions, the number depending on conditions and the tRNA species (Schimmel & Redfield, 1980). At moderate salt concentration and low temperature, Mg^{2+} binding does not appear to be cooperative. Phosphorus NMR studies indicate that the strong binding sites (for Mn^{2+}) are not localized and that bound divalent ions move rapidly about the backbone (Guéron & Leroy, 1980). Proton NMR studies are generally consistent with these conclusions and are ambiguous concerning localization of binding. We presented proton spectra for various Mg^{2+} concentrations [see Johnston & Redfield (1981)]. The present study is primarily concerned with zero, and rather high, Mg^{2+} content per tRNA. The effects of polyamines will be presented elsewhere (J. S. Tropp and A. G. Redfield, unpublished experiments).

NMR studies of exchange rates in zero Mg^{2+} concentration are of some use in developing or confirming hypotheses concerning resonance identification [see Johnston & Redfield (1977, 1978, 1979, 1981), Kearns & Bolton (1978), Römer & Varadi (1977), Robillard & Reid (1979), and Hilbers (1979)]. When identifications have been made, they can then be used to clarify melting phenomena observed by other methods. In particular, low-temperature NMR rate data can be mapped onto high-temperature optical relaxation data (Crothers et al., 1974; Hilbers et al., 1976) by use of temperature-dependent studies and by assuming a single activation energy. In these previous studies, only a single NMR temperature point could be correlated with the extrapolated optical data, whereas in the present work, we could also correlate independently measured activation energies.

Studies of the exchange rate as a function of Mg^{2+} concentration are also useful for identification since they pick out resonances which are magnesium sensitive, in either spectral position or rate, and these are expected to arise from protons near ion binding positions (Bolton & Kearns, 1977). In addition, information on the number of tightly bound Mg^{2+} ions is obtained.

Measurements in the presence of high magnesium concentration are most likely to be relevant for tRNA function. Unfortunately, only a small number of protons show kinetics that can be measured by our more powerful direct methods below the cooperative melt, or before degradation of the sample becomes a problem. Most of the rates below the melting temperature are in a range between 0.005 and 5 s^{-1}, which is inaccessible to NMR measurements at this time.

Other than our own work, and a recent study by Hurd & Reid (1980), prior work has always used line widths and other purely spectral changes to study kinetics. Line-width measurement is difficult and covers only a narrow range of rates. We have introduced two methods for these studies in tRNA which extend the range of rates and permit better determinations of their activation energies. Preliminary descriptions have been published (Johnston & Redfield, 1977, 1978, 1979).

Materials and Methods

Escherichia coli $tRNA^{fMet}$ was the generous gift of Dr. Brian Reid and had been purified from crude tRNA by chromatography on BD-cellulose, DEAE-Sephadex A50, and Sepharose 4B (Reid et al., 1977). Amino acid acceptance was 1.75 nmol/A_{258} unit. It was dialyzed against 2 × 6 L of 10 mM EDTA, pH 4.0, and then 2 × 6 L of glass-distilled water and lyophilized. Both buffers contained 0.1 M sodium thiosulfate. tRNA (140 units) was dissolved in 200 μL of a buffer containing 10 mM EDTA, 0.1 M NaCl, and 10 mM sodium cacodylate, pH 7, and run in a semimicro NMR tube (Wilmad 508-CP) that had been acid washed. The NMR buffer contained 5% D_2O that had been treated with Chelex, and it was Millipore filtered before use.

Yeast $tRNA^{Phe}$ samples were prepared as described in Johnston & Redfield (1981). All buffers were 0.1 M NaCl and 10 mM cacodylate, pH 7, and tRNA concentrations were approximately 1 mM. All samples were dialyzed against the stated buffer in a flow-dialysis microcell. One sample was not sufficiently rigorously dialyzed and contained about 20 mol of total $MgCl_2$ per mol of tRNA, as estimated by comparison of its NMR spectrum with those of samples containing known Mg^{2+} concentrations. We refer to this sample as having about 20 mM total $MgCl_2$ content. A sample which was dialyzed against 15 mM $MgCl_2$ probably contained more than 30 mol of $MgCl_2$ per mol of tRNA and will be referred to as the high Mg sample. Rate measurements were also performed at 37 °C on a sample which was titrated from 0 to 30 mol of $MgCl_2$/tRNA in the presence of 10 mM EDTA, and a series of spectra were obtained on a Mg-free sample to which was added 7 mM EDTA and 15 mM $MgCl_2$.

NMR spectra were obtained as described in Johnston & Redfield (1981). Temperature accuracy is estimated to be ±2 °C. The transverse relaxation rate, or its inverse (T_2), was estimated from the full line width at half-maximum multiplied by π. Apparent longitudinal relaxation rates (henceforth, we call this the "relaxation rate" and denote its inverse by T_1) were measured by a selective saturation–recovery sequence: A long (usually ~100 ms) weak preirradiation at a frequency f_2 was followed by a delay τ and then the 214 observation pulse. The amplitude of the preirradiation was adjusted to saturate only one or a few lines, as determined empirically by observation of the spectrum with τ small. A 2-ms homogeneity spoil pulse followed the f_2 irradiation, to destroy the H_2O signal that the f_2 pulse stimulates, and was always followed by a 3-ms spoil-recovery interval to allow the homogeneity to recover. In later runs, the radio frequency (rf) signal at f_2 was mixed with an audio frequency at f_a to produce irradiation at two separated lines at frequencies $f_2 \pm f_a$, so that relaxation times of both lines could be measured in a single run. An example is given in Figure 1, which also shows the labels we use for lines of the spectrum of yeast $tRNA^{Phe}$, identical with those used in Johnston & Redfield (1981).

It is possible to saturate the entire spectrum with a broad-band frequency-modulated preirradiation that does not saturate the water resonance, and thereby measure the relaxation time of all lines simultaneously. We generally use the selective, rather than the broad-band, saturation–recovery sequence because it permits better resolution of relaxation of individual lines.

The relaxation rates are expected to contain two contributions, one due to interactions with other spins and the other to chemical kinetics:

$$T_1^{-1} = T_{1M}^{-1} + R_1 \quad (1a)$$

$$T_2^{-1} = T_{2M}^{-1} + T_{2K}^{-1} \quad (1b)$$

The magnetic contribution T_{1M}^{-1} arises from cross-relaxation of energy with neighboring protons, from where it is dissipated

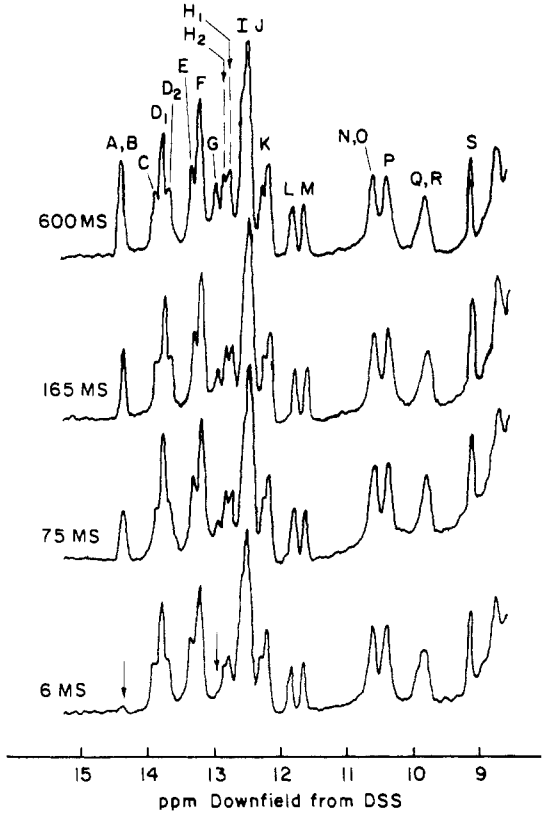

FIGURE 1: Pinpoint saturation–recovery run (partial data) for peaks A + B and G of 1 mM yeast $tRNA^{Phe}$ in the presence of 10 mM EDTA and 30 mM $MgCl_2$, 37 °C. Irradiation is at the points marked by arrows (bottom) by use of a radio frequency mixed with an audio frequency as described in the text. Delays after irradiation are marked on the spectra. Sample volume is 200 μL, and time required is about 4 h, for six time points. The spectral lines referred to in the text are marked on the top spectrum (see also Figure 4).

by further cross-relaxation with further spins. The magnetic contribution to the line width, T_{2M}^{-1}, is from magnetic dipolar broadening by neighboring spins, either other protons or ^{15}N in the case of ring nitrogen protons. Both T_{1M} and T_{2M} are expected to vary weakly with temperature, so R_1 and T_{2K}^{-1} are derived from the observed rates by subtracting from them the values of T_1^{-1} and T_2^{-1} at 20 °C, where the kinetic rates are negligible and the observed rates are nearly temperature independent.

The quantity R_1 in eq 1a is assumed to be the solvent exchange rate. We will call measurement of exchange by selective saturation, and the use of eq 1a to correct for magnetic relaxation, the *saturation–recovery* method of rate measurement. In this method, in effect, the spins "recover" from presaturation by being replaced with solvent spins which were not saturated.

In most cases, the extra kinetic line-width contribution, T_{2K}^{-1}, is also expected to equal R_1, and we call this the *line-width* method of rate measurement. Later, we will briefly discuss when T_{2K}^{-1} is not equal to R_1. The line-width method is limited by the signal-to-noise ratio and spectral overlap to rates between about 100 and 200 s^{-1}. This means that the temperature must often be so high that the tRNA has appreciably unfolded.

We have also estimated R_1 at low temperature by rapidly changing the solvent from H_2O to D_2O and observing those resonances of imino protons which exchange in more than a few minutes (Johnston et al., 1979). We call this the *real-time* method. It is limited to the relatively few protons (about five) which exchange slowly enough to remain after a few minutes.

Theory

We outline the results of NMR theory (Crothers et al., 1974) relevant to this study directed toward the nonspecialist reader. Experts will recognize some assumptions and oversimplifications introduced for the sake of brevity and readability; we will mention some of these where they may be important or questionable.

The simplest model for proton exchange (Englander & Englander, 1978; Hilbers, 1979) is symbolized by the reaction scheme

$$\text{closed} \underset{k_{cl}}{\overset{k_{op}}{\rightleftharpoons}} \text{open} \xrightarrow{k_x} \text{solvent} \qquad (2)$$

Here "closed" represents the native form of tRNA, "open" is unfolded tRNA, and k_x is the rate of solvent exchange from the open species. This scheme is clearly an oversimplification since different parts of the molecule open at different rates. Also, it is by no means clear that there is only one "open" state; perhaps at low temperature, the dominant pathway involves some partially open state. It is also conceivable that proton exchange occurs directly from the "closed" state. However, lacking more information, we will use this scheme as a working model and assume that in the "open" state the imino proton is exposed to solvent and that the closed–open reactions are the ones observed by optical and calorimetric methods.

Our interpretation of our data can be stated very simply: Except where we explicitly say otherwise, we believe the rate R_1 is nearly equal to k_{op}. This is predicted by eq 2 if $k_x \gg k_{cl}$, so that k_{op} is rate limiting, for the saturation–recovery and real-time methods. These methods are equivalent to tritium-exchange measurements, provided, in the case of the saturation–recovery method, that the subtraction of T_{1M}^{-1} can be made reliably. Estimates of k_x, for ring nitrogen protons on free bases at pH 7, are in the range of 10^5–10^6 s^{-1} at 20 °C, and these rates are presumably higher at the temperatures where we make most of our measurements. Estimates for k_{cl} are generally less than 10^3 s^{-1} except for the highest temperature transitions.

One case where R_1 may not equal k_{op} is for real-time measurements below room temperature (Johnston et al., 1979). In that case, the relatively low activation energy suggests a change in mechanism, perhaps involving direct solvent exchange via diffusion from the closed state, or opening of single base pairs.

The line-width method also measures R_1, provided that $k_{cl} \lesssim 2\pi|f_{op} - f_{cl}|$, where f_{cl} is the NMR frequency of the line in question for the closed states and f_{op} is that either for the open state or for H_2O, depending on considerations which we need not discuss. The frequency shift $f_{op} - f_{cl}$ is likely to be at least 1 ppm, or 270 Hz, for most exchangeable protons except possibly those on unpaired bases, and this condition is generally obeyed.

By adding exchange catalysts which are expected to affect k_x and not k_{op}, one can attempt to establish whether k_{op} is rate limiting or not. This has been done by others for various cases (Mandal et al., 1979), including tRNA at high temperature (Hurd & Reid, 1980), and the result has been that R_1 is indeed opening limited for all double helixes studied so far, for ring N protons.

Finally, we consider line intensities. Spectral lines will become relatively indistinct in the spectrum when R_1 becomes a few times the magnetic line width T_{2M}^{-1}. Thus, for practical purposes, they will seem to disappear. We call this kind of disappearance an *NMR melt*.

Spectral lines will also disappear when the equilibrium constant $K = k_{cl}/k_{op}$ becomes appreciably less than one, even

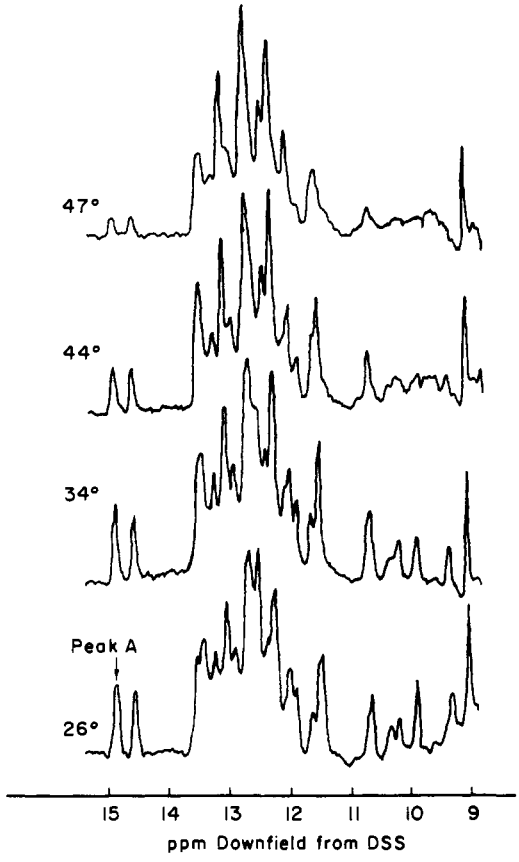

FIGURE 2: Low-field NMR spectra of *E. coli* $tRNA^{fMet}$ in zero $MgCl_2$ concentration as a function of temperature. Buffer was 0.1 M NaCl, 10 mM EDTA, and 10 mM sodium cacodylate, pH 7.0.

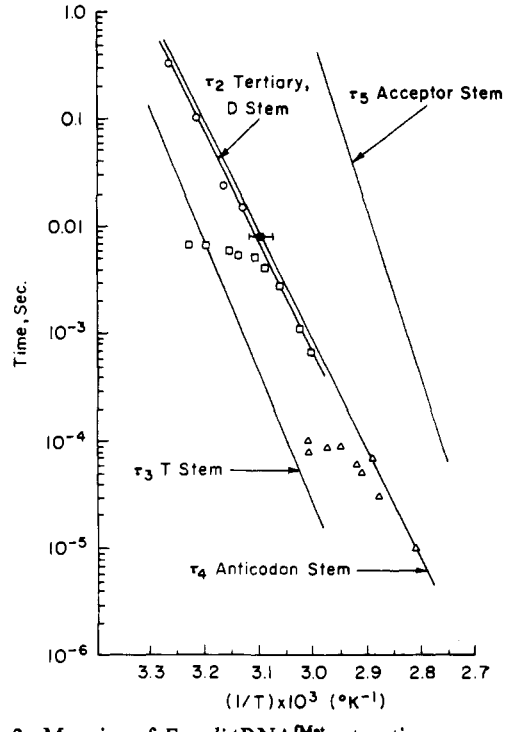

FIGURE 3: Mapping of *E. coli* $tRNA^{fMet}$ saturation–recovery rates for peak A (corrected by subtracting a magnetic rate of 10 s^{-1}) onto optical temperature-jump data of Crothers et al. (1974). (○) This research; (□) T-jump data assigned to tertiary and D-stem unfolding; (△) T-jump data assigned to anticodon unfolding; (■) NMR point from Crothers et al. obtained by line broadening of peak A.

if there is not important kinetic broadening. We believe this occurs for a few resonances, and we will call such a disappearance an *equilibrium intensity loss.*

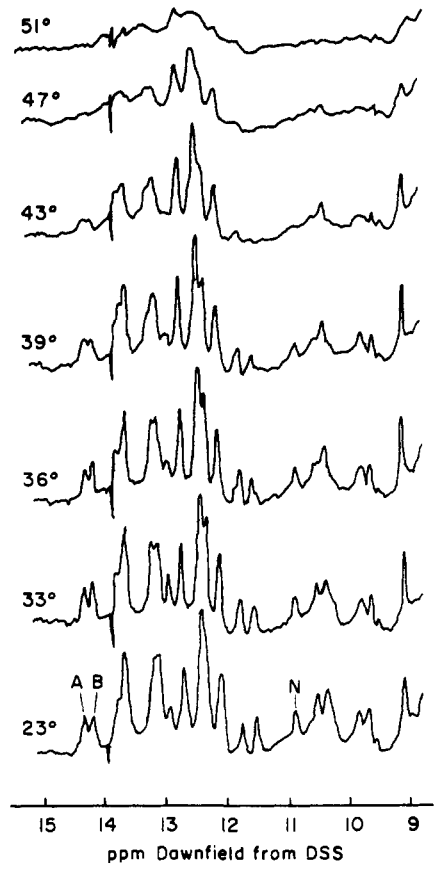

FIGURE 4: Temperature dependence of the resolved low-field proton resonances of yeast $tRNA^{Phe}$ in the absence of $MgCl_2$. The $tRNA^{Phe}$ was dialyzed against a buffer containing 10 mM EDTA, 0.1 M NaCl, and 10 mM sodium cacodylate (pH 7). The spectra from 23 to 33 °C are the result of 10 000 free induction decays while those taken at 36 °C and above are the result of 16 000 free induction decays. All spectra are plotted to correct for the differences in these numbers. The specific activity of the yeast $tRNA^{Phe}$ was 1.8 nmol of Phe/A_{258} unit of tRNA, and the NMR sample contained 105 A_{258} units of $tRNA^{Phe}$ in 180 μL of buffer. Peaks A, B, and N are marked in the bottom spectrum; see Figure 1 (top) for other spectral lines.

Results

E. coli $tRNA^{fMet}$. Early events in the thermal melting of this species in zero $MgCl_2$ concentration are shown in Figure 2. Reversibility of the melt was established by running a spectrum at the end of this series after returning to low temperature. We report on limited kinetic data from this sample for peak A which has been reliably assigned to the NH–N proton of the reverse Hoogsteen tertiary interaction sU8–A14 (Daniel & Cohn, 1975; Wong et al., 1975; Robillard & Reid, 1979). It appears from Figure 2 that this peak decreases in intensity by more than 50% before any broadening is observed, implying an equilibrium intensity loss.

This conclusion was confirmed by saturation–recovery measurements on peaks A, between 4 and 47 °C. From 4 to 31 °C, the observed rate is 10 ± 1 s^{-1}, and we assume that this is due to magnetic cross-relaxation. This rate was subtracted from rates observed from 34 to 47 °C, and the inverse of the result was plotted in Figure 3, as a proton exchange time. Also plotted in Figure 3 are exchange time and optical relaxation time data reported for two transitions of the same tRNA obtained under similar conditions (Crothers et al., 1974). Note that the coordinates in Figure 3 are essentially reversed relative to those we use in later figures, to conform to the presentation of Crothers et al.

Yeast $tRNA^{Phe}$. Spectra obtained at zero, and moderate, $MgCl_2$ concentration are shown for various temperatures in

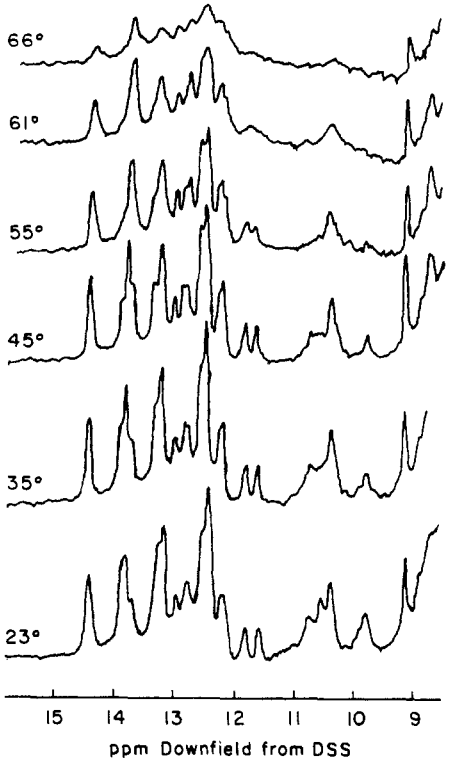

FIGURE 5: Temperature dependence of the NMR spectra of yeast $tRNA^{Phe}$ in the presence of low $MgCl_2$ concentration. The tRNA/$MgCl_2$/EDTA ratio is 1:15:7. Temperatures are marked.

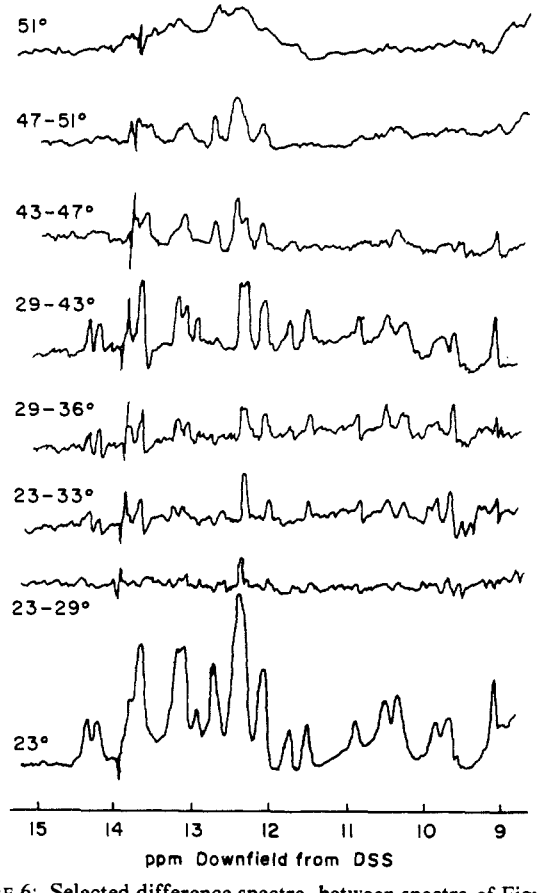

FIGURE 6: Selected difference spectra, between spectra of Figure 2 and others obtained in the same run, for yeast $tRNA^{Phe}$ in zero $MgCl_2$ concentration. For reference, 23 and 51 °C spectra are included. All plots are at the same gain.

Figures 4 and 5. Selected difference spectra are shown in Figures 6 and 7.

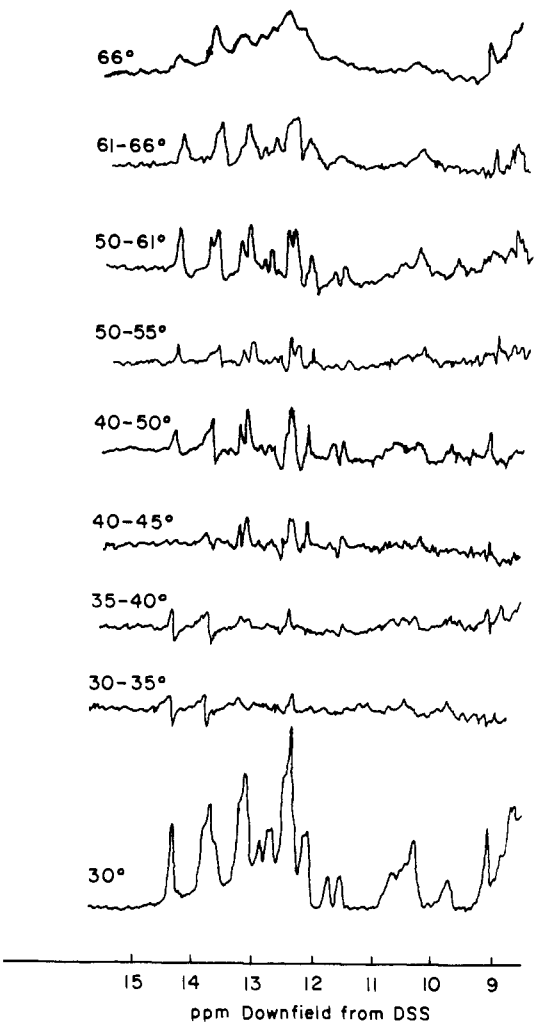

FIGURE 7: Selected difference spectra, between spectra of Figure 3 and others obtained in the same run, for yeast $tRNA^{Phe}$ in 15 mol of added $MgCl_2$ per mol of tRNA, and 7 mM EDTA. For reference, end spectra are also included.

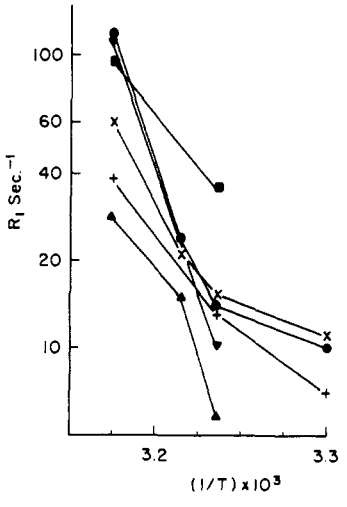

FIGURE 8: Exchange rates for protons having resolved or partially resolved resonances in yeast $tRNA^{Phe}$ at zero $MgCl_2$ concentration. (●) Peak A, secondary AU, possibly UA6; (×) peak B, probably U8–A14; (+) peak C, possibly AU5; (■) peak G, possibly G19–C56; (▲) peak L, U69 of the pair GU4; (▼) peak M, unassigned. Lines connecting data points are for the reader's convenience.

Spectral data at various temperatures were also taken on the high $MgCl_2$ sample (dialyzed against 15 mM $MgCl_2$), and on the moderate $MgCl_2$ sample containing 1 mM EDTA and a probable Mg/tRNA ratio of about 20:1 (see Materials and

Table I: Exchange Rates for Composite Imino Resonances of Yeast $tRNA^{Phe}$ in Zero Mg^{2+} Concentration[a]

peak	tentative assignment[b]	temp (°C) 30	36	42
D	AU52, UA12/AU7	+/10	+/20	35/gone
E	m^7G46-G22	20	30	gone
F	11, 29, 50	+/15	+/35	7/120
H	GC10	+	7	10
I	?/GC1	+/50	+/gone	–
J	secondary GC	+	5/20	10/45
K	CG13/G15C48	+/20	+/20	7/gone

[a] tRNA (1 mM) in 0.2-mL volume with 10 mM cacodylate, pH 7, 10 mM EDTA, and 0.1 M NaCl. Saturation-recovery rates in s^{-1}, corrected for magnetic relaxation by subtracting 5 s^{-1}. (+) means data taken but rate not significantly different from zero (<5 s^{-1}). (–) means no data taken. Slash means biphasic relaxation with the indicated rates. [b] See Johnston & Redfield (1981) for discussion.

Table II: Exchange Rates of Imino Protons of Yeast $tRNA^{Phe}$ at 37 °C as a Function of the Total Mg/tRNA Ratio[a]

peak	tentative assignment	Mg/tRNA 0	1	4	10	30
A	UA6	20	20	10	+	+
B	U8-A14	15	10			
G	G19-C56	35	5	+	+	+
L	U69	10	10	5	5	5
M		30	15	10	+	+
N	ψ55 N1	70	20	10	15	20
O		–	–	200	20	
P	G4, m_2^2G26	–	–	10	5	5
Q		30	25	15	25	5
R		25	60	30		

[a] Initial conditions were about 1 mM tRNA, 10 mM EDTA, 0.1 M NaCl, and 10 mM sodium cacodylate. Concentrated $MgCl_2$ was added successively to yield final 6% dilution. Other conditions and notations were as described in Table I.

Methods). No important temperature-dependent spectral differences were found between these samples and that used to obtain Figures 5 and 7.

Relaxation rates in zero Mg concentration are plotted in Figure 8 for several resolved resonances; those for overlapping resonances are summarized in Table I.

All saturation–recovery measurements leveled off around room temperature at a magnetic rate of 4–9 s^{-1}. To correct for this magnetic contribution, we have subtracted 5 s^{-1} from all yeast $tRNA^{Phe}$ rates in this paper to obtain R_1, as discussed above. The maximum error in this procedure is likely to be 5 s^{-1}.

We have studied saturation–recovery rates at moderate and high $MgCl_2$ concentrations up to 50 °C. For almost every peak in the spectrum, the observed rates are nearly temperature independent in the presence of $MgCl_2$ up to 50 °C, suggesting that magnetic relaxation dominates and that the solvent exchange rate is less than 5 s^{-1} for most imino protons. Exceptions to this are peaks A or B, C, and L and components of E and F. Rates for these peaks are summarized in Figure 9, which also shows limits for exchange of typical imino protons inferred from line width, saturation–recovery, and real-time measurements and rates for the most slowly exchanging protons observed by the real-time method. The only clear difference between rates for moderate and high $MgCl_2$ concentrations is that exchange for a component of peak E is much slower at high $MgCl_2$ concentration than at moderate $MgCl_2$ concentration. Table II shows the results of saturation–recovery measurements as a function of $MgCl_2$ concentration,

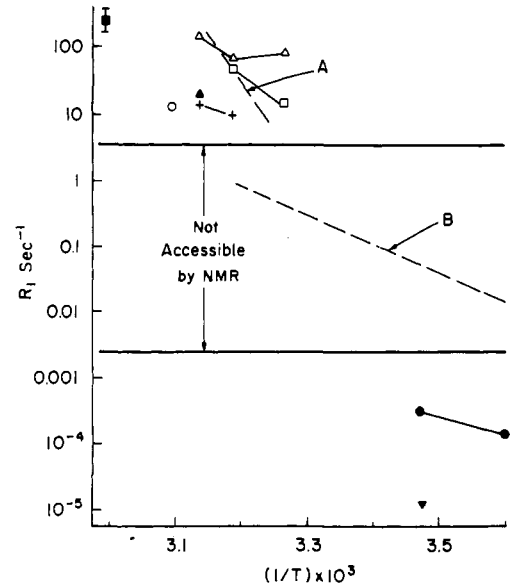

FIGURE 9: Exchange rates for various ring nitrogen protons of yeast $tRNA^{Phe}$ in the presence of magnesium. For comparison, dashed lines indicate results in zero magnesium concentration: (A) typical tertiary proton (see Figure 8), activation energy 65 kcal/mol; (B) poly(rA-rU) ring N protons as reported by Mandal et al. (1979). Data obtained in samples dialyzed against 15 mM $MgCl_2$ are denoted by solid symbols; other points were obtained with approximately 20 mM total $MgCl_2$. (■) Typical secondary GC, from line width; (▼) UA12 and (●) most stable secondary GC (in unfractionated tRNA), by real-time observation. Saturation–recovery measurements: (○) peak A–B, U8–A14 and possibly UA6; (△ and ▲) component of peak E, possibly m^7G46; (+) peak L, U69 of the pair GU64; (□) component of peak F, possibly Aψ31.

in the presence of 10 mM EDTA at 37 °C. Two spectra from this titration were also shown in Johnston & Redfield (1981).

Interpretation. (*a*) *E. coli* $tRNA^{fMet}$. The data of Crothers et al. (1974) shown in Figure 3 measure the relaxation time τ_r where, for a two-state model, τ_r^{-1} is $k_{op} + k_{cl}$. These workers assumed that k_{cl} is much less strongly temperature dependent than k_{op}, and thereby estimated a melting temperature of 47 °C where $k_{op} = k_{cl}$, and an activation energy of 50 kcal/mol for k_{op} for tertiary melting. The solid line marked "tertiary" is extrapolated from the optical data for the tertiary transition by using this activation energy. Extrapolated opening times obtained in the same way for other optical transitions are also shown.

The exchange rate for the ring N proton of uracil monomer was estimated by us from the NMR line width under the same buffer conditions to be 5×10^3 s^{-1} at 25 °C (unpublished experiments). This rate should increase with temperature. Since it considerably exceeds the inverse of the optical relaxation time (Figure 3), exchange will not be rate limiting, and within the framework of eq 2 the plotted NMR τ is then expected to be the inverse of k_{op}. It is seen that the NMR rates agree well with the expected opening time k_{op}^{-1} extrapolated by Crothers et al. (1974) from above the melting temperature. Thus, our data are consistent with the optical data and its interpretation, based on eq 2, and the assumption that the NMR rate measures k_{op} rather than some other kinetic process.

In fact, the NMR rates are nearly consistent with extrapolation from another optical transition with a melting temperature of 70 °C (Figure 3). However, as indicated in Figure 2, the transtion reported by resonance A has a melting temperature much lower than this since the integrated intensity of this resonance decreases above 40 °C. Since this appears to be an equilibrium intensity loss, the NMR intensity variation

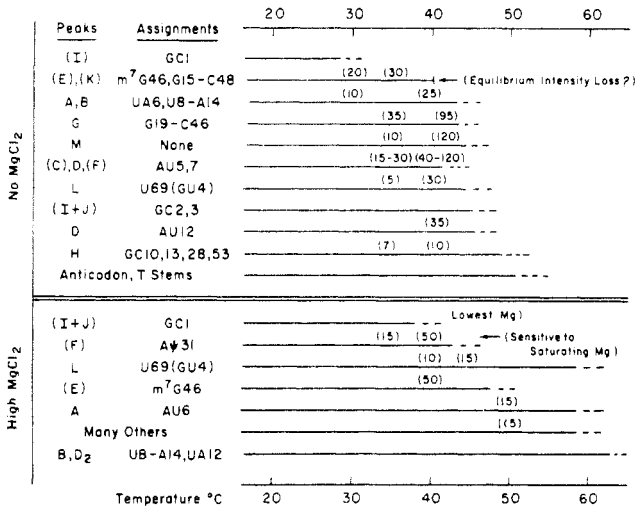

FIGURE 10: Schematic summary of unfolding events observed by means of NMR. The numbers in parentheses are approximate exchange rates for the different peaks. The horizontal lines indicate the range over which lines are reasonably observable, and the dashed ends indicate the temperature at which a line becomes unobservably broadened by solvent exchange ($R_1 \lesssim 200\ s^{-1}$). The assignments are not firm in many cases, as is described in the text. Peak labels in parentheses denote composite peaks for which identification is especially speculative. Data obtained with magnesium are for less than saturating Mg^{2+} concentration, about 20 ions per tRNA (about 20 mM total $MgCl_2$ content), except as indicated.

indicates that the melting temperature is 45 °C, in excellent agreement with the optical estimate by Crothers et al. of 47 °C for the transition they assign to tertiary unfolding.

(*b*) *Yeast tRNA^{Phe}.* We now present a partial description of the unfolding sequence of this species as the temperature is raised. This picture is consistent with an orderly unfolding sequence and with the assignments given in Johnston & Redfield (1981), but this consistency is not a strong indication of the correctness of our picture. Uncertainties in assignments were discussed in Johnston & Redfield (1981). Measurements at higher field should improve the quality of the relaxation data and revise some conclusions. Figure 10 summarizes the sequences of unfolding described in the following sections.

Below 30 °C under our conditions, we have no indication of multiple conformers as has been inferred from fluorescence by Ehrenberg et al. (1979) for modified yeast tRNA^{Phe} in 0.1 M KCl at pH 7.5. If there is a second conformer present, we estimate its concentration as less than 20% of the dominant one. We cannot prove that rates which we measure at higher temperatues are not due to a fairly high-abundance ($\lesssim$20%) second conformer for which exchange is rapid, but except for disappearance due to tertiary structure changes around 45 °C (equilibrium intensity loss) we do not interpret our results in this way.

Unfolding Sequence with Zero Magnesium Concentration. The first event in thermal unfolding is a small change in the shape of the complex peak I + J and the appearance of a rapidly relaxing component in it (Table I and Figure 6, 23–29 and 23–33 °C spectra). It appears that this involves a single proton which is undergoing an NMR melt at about 33 °C. The most straightforward candidate for this proton is that of GC1, for which low-temperature melting seems likely as an end-fraying effect; this is also reasonable because disruption of the GC1 base pair might lead to minimum perturbation of the rest of the structure and the spectrum. It seems likely that the CG2 imino resonance would be shifted several tenths of a part per million if GC1 were fully disrupted, and there is no sign of such a shift. Presumably, GC1 remains stacked most of the time well beyond its apparent NMR melting point. Thus, the disappearance of GC1 is probably a purely kinetic effect, with a relatively rapid k_{cl}, so that the equilibrium constant $K = k_{op}/k_{cl}$ for GC1 remains small up to at least 40 °C.

At slightly higher temperatures, several resonances start to show observable exchange kinetics; we assume these are tertiary resonances and discuss them as groups of similar resonances with similar behavior. First are two resonances which are components of lines E and K. The imino proton of the m^{7}G46–G22 tertiary interaction has been assigned rather solidly to peak E (Hurd & Reid, 1979), but the kinetic effect we see at this point could be due to another overlapping resonance. Resonance K is assigned to G15–C48 on the basis of paramagnetic ion broadening studies (B. Reid, unpublished experiments) and Mg-induced recovery of lost intensity at high temperature [see Johnston & Redfield (1971)], but this assignment is tenuous. These resonances are unusual in that their exchange rates show weak temperature dependence, and they seem to disappear from the spectrum at a temperature where the rates are too small to produce much broadening (i.e., <10 Hz), suggesting an equilibrium intensity loss (as defined under Theory) produced by some conformation change at about 40 °C. This conclusion is highly tentative in view of the complexity of the lines in question; there is the possibility that a shift occurs which gives the appearance of an intensity loss.

A second pair of resonances which show remarkably similar behavior are the two most downfield, A and B. Peak A is a secondary AU ring proton resonance, as shown by Sanchez et al. (1980), and was tentatively assigned in Johnston & Redfield (1981) to UA6, and peak B is from a reverse Hoogsteen base pair generally believed to be U8–A14. These resonances show observable kinetic exchange at 30 °C, with a fairly high activation energy (20–60 kcal/mol). The Arrhenius plot of rates for these protons is not a straight line, suggesting some change in mechanism, but this conclusion is tentative in view of possible experimental error.

Peak G shows peculiar behavior in that its rate increases from unobservable to about 35 s^{-1} from 30 to 36 °C, and then it changes relatively slowly between 36 and 42 °C to 100 s^{-1}. It was assigned to the tertiary Watson–Crick pair G19–C56 at the corner of the molecule which caps the composite acceptor–T-stem helix. This is a tentative assignment, and Aψ31 is another possible candidate for it.

The mostly unidentified resonances between 12 and 9 ppm disappear somewhat before the secondary imino protons (Figure 4). Of these, only peaks L and M were studied by saturation–recovery, except at 37 °C. Peak L is assigned to U69 of the acceptor GU4 base pair, and M is unassigned. The acceptor melt will be discussed later.

The remaining resonances in the 9–12-ppm region show exchange more rapid than that of peak L. G4 and m$_2^2$G26 are in this region (both at 10.4 ppm) but cannot be distinguished from other peaks.

It is striking that at the highest temperature studied, 40 °C, several resonances which are attributed to important tertiary protons show similar rates, of the order of 100 s^{-1}. This could be the rate for major unfolding of the tertiary structure at this temperature.

In this connection, peak S, reliably assigned to the C8 proton of m^{7}G46 on the basis of chemical modification (Hurd & Reid, 1979) and NOE [see Johnston & Redfield (1981)], is of interest. This proton exchanges in several hours, so $R_1 = 0$ for our time scale. At 45 °C, it is just beginning to broaden by about 8 Hz, corresponding to a kinetic contribution T_{2K}^{-1} of 25 s^{-1} to the transverse relaxation rate. If the parameter $2\pi f_{op}$

$-f_{cl}|/k_{cl}$ discussed under Theory is greater than 1, then T_{2K}^{-1} should equal k_{op}. This yields a smaller value of k_{op} than that reported by resonance E, and assigned to the imino proton of the same base. It is possible that the assignment of the exchanging imino proton is wrong or that the process which allows the imino proton to exchange does not affect the C8 proton line width and that the C8 proton reports some other process. Equally likely is the possibility that broadening of this resonance should be treated by using the rapid-exchange limit. This limit requires that the above parameter be less than 1, and if so, the extra line width is predicted to be

$$T_{2M}^{-1} = [2\pi(f_{op} - f_{cl})]^2 K/k_{cl} \quad (3)$$

provided $K = k_{op}/k_{cl}$ is small compared to unity. Equation 3 is a special case of the standard line-width formula $T_2^{-1} = \langle\Delta\omega^2\rangle\tau_c$ where $\Delta\omega = \omega - \langle\omega\rangle$ is the deviation of the time-varying angular resonance frequency from its average, $\langle\omega\rangle$, the brackets detone time average, and τ_c is the correlation time for the frequency shift. In the present case, if $K \ll 1$, $\langle\omega\rangle \cong 2\pi f_c$ and $\langle\Delta\omega^2\rangle$ is equal to the square of the shift in angular frequency upon unfolding times the fraction of time K spent unfolded. The correlation time τ_c is the mean time spent unfolded, which is k_{cl}^{-1}.

At 45 °C, k_{op} might reasonably be 100 s^{-1} as is found for several tertiary resonances, and T_{2K}^{-1} is estimated from the line width to be 25 s^{-1}. Thus, eq 3 would require that $2\pi|f_{op} - f_{cl}|/k_{cl}$ be about 0.5. A reasonable and consistent estimate for k_{cl} is several hundred per second so $f_{op} - f_{cl}$ would have to be less than about 100 Hz, which is possible. Under these rapid-exchange conditions, the line should shift as K approaches unity, and its frequency should be the weighted average $f = (f_{cl} + Kf_{op})/(1 + K)$. There does appear to be a slight upfield shift of peak S at 47 and 51 °C (Figure 4). A downfield shift might have been expected from the observed position of this resonance for m^7G monomer dissolved in dimethyl sulfoxide (Hurd & Reid, 1979), but its position in unfolded tRNA may be affected by the fact that m^7G is formally positively charged. If these assumptions involving fast exchange are valid, then the equilibrium for the transition being reported is somewhat above 50 °C.

We now summarize transitions which we attribute to breakdown of secondary structure. The first of these is unambiguously signaled by the definite instability of the GU base pair which is in the acceptor stem, correlated with other apparent secondary changes which we also attribute to the acceptor stem. It is unexpected that a relatively long helix like the acceptor (three AU and three GC pairs separated by GU4) would be less stable than the other, shorter, helixes. Perhaps the GU pair forms a weak link (Romaniuk et al., 1979) which effectively buffers the three AU pairs from the GC triple. Presumably, lack of a closed end also contributes to relative instability. The D stem may be relatively stable, despite its short length, because of its involvement in many tertiary interactions.

The unfolding of the acceptor stem apparently occurs in several steps. First observable at 30 °C is relatively rapid opening of GC1, probably with even more rapid closing so that the base is closed most of the time and CG2 is not much destabilized, as we already proposed. At the same temperature, the three AU pairs 5–7 start to open, but less rapidly.

Components of peaks C and D, that we previously assigned to AU5 and AU7, show rates similar (within a factor of two) to those of peak A, assigned to UA6. These rates cannot be measured as accurately as those for peaks A and B because C and D are composite. These saturation–recovery data support the assignment of the three acceptor AU pairs to peaks A, C, and D as proposed in Johnston & Redfield (1981). Similar early exchange due to CG2 and GC3 is not resolved for peaks I + J, where these resonances are expected, but such components might be obscured for these complicated lines. There is an intensity loss in this region at about 40 °C [see Johnston & Redfield (1981) for a discussion]. By 42 °C, there is a substantial difference between the acceptor rates and those for tertiary interactions, which are about twice as fast.

This picture of acceptor unfolding is somewhat speculative, and that for the other stems is more so. At 43 °C, it appears that the D, T, and anticodon stems are intact and that their imino protons are exchanging at a rate of less than about 40 s^{-1} so that their resonances are not melted, whereas the acceptor and tertiary imino protons are exchanging rapidly, and the associated structures are approaching disintegration. The next secondary feature to melt may be the D stem, signaled by saturation–recovery rates observed at 43 °C of about 10 s^{-1} for candidates for the three GC pairs and 34 s^{-1} for AU12, of this stem. The highest temperature spectrum, at 51 °C, resembles the spectra of the T stem and the TψC-loop fragment reported previously (Lightfoot et al., 1973), so that this may be the last feature to melt at high temperature. However, there seems to be unexpectedly high intensity in peak H at the highest temperature which is not easily rationalized in terms of these assignments.

Unfolding Sequence with $MgCl_2$. As expected, magnesium raises the temperature at which major NMR changes occur, and it shifts most of them to a single cooperative transition, around 60 °C. However, some changes are discernible both below and above this temperature.

Real-time observation of exchange is possible for several imino protons at low temperature in the presence of Mg^{2+}, whereas it is not possible in the absence of Mg^{2+} because all imino exchange rates are too large (N. Figueroa, unpublished experiments on unfractionated tRNA). Some real-time data from Johnston et al. (1979) are included in Figure 9 to illustrate the low activation energy for exchange at these temperatures. Thus, as we already mentioned, exchange rates at these temperatures are likely to be determined by some process other than unfolding of a major part of the structure, which most likely governs the high-temperature rates. Since the bulk (>75%) of the secondary protons exchange in less than 5 min, this change in mechanism is nearly universal, but we do not have any useful proposal for what it might be.

Real-time exchange measurements report especially stable regions of the molecule, but we have used this property in reverse to identify an extremely slowly exchanging resonance with the section of the molecule that we expect to be most stable, namely, UA12 in the D stem. However, one resonance that has been identified independently shows unusually slow exchange, namely, that at 12.9 ppm (peak G) assigned to G19–C56 (Johnston et al., 1979). This assignment is not firm, being based on a ring-current calculation and on the moderately early melting of this resonance in zero Mg^{2+} concentration (rate 35 s^{-1} at 35 °C). The least that can be said is that one of the less labile protons in zero Mg^{2+} concentration becomes one of the most stable in the presence of Mg^{2+}, and G19–C56 is a reasonable identification for it. This base pair is at the corner of the molecule, and it caps the long stack of base pairs which combines the acceptor and T-stem helixes. It is presumably stabilized by a Mg^{2+} ion coordinated directly to the phosphate of G19 and by hydrogen bonding via H_2O to the bases G20, U59, and C60. Further stabilization is likely from the Mg^{2+} directly coordinated to the phosphates of G20 and A21.

There is an inaccessible range of rates between the real-time and the other measurement methods that we use (0.01–10 s^{-1}). Most of the downfield protons remain stable with exchange rates in this range all the way to 55 °C, and only a few show measurable exchange or broadening much below this temperature. We did not make studies above 50 °C with $MgCl_2$ in much detail because of expected Mg-catalyzed hydrolysis of the sample.

Two features seen below 50 °C are most likely isolated events. One is the disappearance of some intensity in the large resonance I + J, between 30 and 40 °C (see Figure 7, 35–50 and 30–50 °C difference spectra). We tentatively assign this kinetic event to end fraying of GC1, as we did for the similar transition between 23 and 33 °C in zero Mg^{2+} concentration. It was observed only for the sample containing the least total $MgCl_2$ (tRNA/Mg/EDTA 1:15:7). The other feature is the relatively rapid exchange with low activation energy for a peak which is attributed very tentatively to the Aψ31 imino proton [part of peak F; see Johnston & Redfield (1979)]. We assumed that this peak was missing from spectra taken in zero Mg^{2+} concentration due to exchange broadening. It also appeared to be missing from the sample containing the least bound Mg^{2+} (15 mM total $MgCl_2$ concentration and 7 mM EDTA). In the other two $MgCl_2$-containing samples, increased exchange was observed for a component of peak F below 50 °C, and one proton's intensity is lost from this peak by 50 °C.

The GU base pair of the acceptor stem also shows early imino exchange kinetics, less rapid than at zero Mg^{2+} concentration but more rapid than for secondary base pairs in the presence of $MgCl_2$. The activation energy for GU imino exchange is low, as can be estimated from saturation–recovery measurements at 40 and 34 °C, and it does not broaden noticeably until the cooperative melt, between 50 and 60 °C.

Two other resonances show early exchange kinetics below 50 °C, namely, resonance intensity at peak E, assigned to the m^7G46–G22 interaction, and a component of peaks A and B, which coincide at high Mg^{2+} concentration. The rapidly exchanging component of peaks A and B is most probably peak A because in the $MgCl_2$ titration study (Table II) this peak shows the more rapid exchange kinetics, as compared to peak B, for equimolar $MgCl_2$ added. Resonance A was shown to be a secondary AU pair (Sanchez et al., 1980) and was assigned in Johnston & Redfield (1981) to AU6. AU5 would have been a more natural assignment for peak A, and be more plausible as a less stable base pair, but it was assigned to peak C on the basis of a weak nuclear Overhauser effect.

The relative instability of the m^7G46–G22 interaction (part of peak E) may conceivably report relative motion of the two major stacks of the molecule. This kinetic process is the only one which is slowed dramatically when the sample is saturated with $MgCl_2$ (dialysis with 15 mM $MgCl_2$) as compared with smaller levels of $MgCl_2$ (Figure 9).

The $MgCl_2$ titration study at 37 °C (Table II) is consistent with these temperature studies. As we just mentioned, it indicates which of the two peaks A and B, that coincide at high Mg^{2+} concentration, is the rapidly exchanging one, namely, peak A. For a 1:1 Mg/tRNA ratio, this peak exchanges twice as rapidly as peak B. In Johnston & Redfield (1981), we mentioned that spectral shifts occur for three ranges of $MgCl_2$ concentration, namely, coalescence of peaks A and B (Mg^{2+}/tRNA $\cong$ 2), appearance of a shoulder on the upfield side of peak D (Mg^{2+}/tRNA = 10), and upfield movement of peak N (saturating Mg^{2+}/tRNA). There are corresponding changes in kinetics: at 37 °C (Table II), for example, lines that are missing from the spectrum for zero Mg^{2+} concentration reappear when Mg^{2+} is added in the ratio Mg^{2+}/tRNA = 2 and also 10. A component of line E, tentatively identified as m^7G46–G22, is sensitive to higher Mg^{2+} concentration, at higher temperature (Figure 9).

The Mg-containing sample with the smallest bound $MgCl_2$ (Mg/EDTA/tRNA 15:7:1) was not surveyed by saturation–recovery but was studied spectrally over a wide temperature range. Between 40 and 50 °C, it shows a spectral transition resembling that occurring below 40 °C in zero $MgCl_2$ concentration; compare the 40–50 °C difference spectrum of Figure 7 with the 29–43 °C spectrum of Figure 3 in Johnston & Redfield (1981). This similarity suggests that the acceptor stem melts slightly before the other stems, at least in moderate $MgCl_2$ concentration, as in zero $MgCl_2$ concentration.

The most interesting features of these spectral studies are evident at 61 and 66 °C (Figure 5). Prominently remaining are two peaks at the low-temperature positions of A + B and D. The most straightforward interpretation of this observation is to assign these resonances to U8–A14 (peak B) and UA12 (peak D) and to explain their stability by the persistence of Mg^{2+} in a highly favorable binding site at the sharp bend of the phosphate backbone at residue 10 (Kim, 1978). We suggest that this site and the D stem remain intact up to high temperature, stabilized by a Mg^{2+} ion.

Another striking feature is the persistence of peak G (tentatively G19–C56) up to 61 °C as a sharp peak. This is consistent with the slow exchange found for this peak by real-time studies at lower temperatures, which we already discussed.

Discussion

This research has provided a more detailed picture than previous studies of thermal unfolding processes for any macromolecule. The measurements on *E. coli* $tRNA^{fMet}$ correlate well with optical temperature-jump relaxation studies (Crothers et al., 1974) and suggest that the high-temperature behavior that we measure is the opening rate of major parts of the molecule, with activation energies above 40 kcal/mol. The optical measurements indicate that closing of the structure is slower than exchange from the free base, suggesting that solvent exchange from the unfolded structure will not be rate determining. Many of the resonances for yeast $tRNA^{Phe}$ shown in Figure 6 show exchange rates which extrapolate to the optically estimated tertiary closing rate of about 200 s^{-1} (Urbanke et al., 1975) at 43–47 °C, which is approximately the temperature of the lowest major calorimetric melt seen under similar conditions for this tRNA (Privalov & Filimonov, 1978). The low-temperature real-time measurements in the presence of magnesium suggest a change of exchange mechanism since the activation energies of observably exchanging peaks are low, and those of protons that were not observed because of too rapid exchange must also be low (otherwise they would not exchange rapidly at room temperature).

Our data generally complement calorimetric data on tRNA. In high magnesium concentration, we confirm the nearly cooperative melting around 60 °C that is seen calorimetrically, and we also see evidence for some structure extending to higher temperatures. The NMR spectra suggest that in yeast $tRNA^{Phe}$ this structure is the D stem and U8–A14 tertiary interaction. Below the transition at 60 °C, we see little exchange, but one resonance which may be that of the imino proton of m^7G46 reports some motion. In addition, the GU4 base pair shows detectable instability below 60 °C. Thus, these could be sites of functionally important flexibility. The extreme stability of a few base pairs at room temperature in high

magnesium concentration may indicate unusual rigidity of some part of the molecule, probably around the D stem.

We interpret the initial melting which we see in zero magnesium concentration as do others, in terms of melting of the tertiary structure. However, our interpretations of other later features of melting are different from those of previous workers. The most similar conditions used by previous workers were those of Privalov & Filimonov (1978), namely, 0.157 M Na^+, compared to 0.13 M in this work. The sequence and temperatures of our NMR-deduced transitions agree qualitatively with the results of their calorimetric measurements (five transitions between 41 and 79 °C) although we cannot estimate the highest temperature transition. The lowest temperature transition after the tertiary melt was interpreted by these workers as that of the D stem, whereas we believe it is the acceptor stem, based on melting of the GU interaction and the nearly simultaneous increase of rate for about three secondary AU pairs. We assigned melting of the remaining three stems very tentatively in the order D stem, anticodon, and T stem, whereas Privalov and Filimonov assign the order of secondary melting as D stem, acceptor stem, T stem, and anticodon stem. The most important difference between these interpretations is in the acceptor stem, signalled in our work by the melting of GU4 and several AU pairs. The possibility must be considered that the GU pair is inherently unstable but that the rest of the acceptor remains intact so that use of GU stability as an assay for acceptor stability is misleading. However, in *E. coli* $tRNA^{Val}$, we find that in zero Mg^{2+} concentration GU49 (second pair from the open end of the T stem) is as thermally stable as a typical secondary pair (unpublished experiments), supporting our interpretation of the GU4 exchange data.

An optical T-jump study at 0.02 M Na^+ also led to assignments of melting in the following order: tertiary structure followed by the acceptor and anticodon stems, then the T stem, and finally the D stem (Coutts et al., 1975). As expected, all transitions were shifted to lower temperature. This interpretation is close to ours, but the salt concentration was significantly lower than that used in our work.

It appears that NMR can supply a more specific picture of melting than other techniques, insofar as resonances can be resolved and identified. We are progressing steadily in making assignments, and higher field magnets and nuclear Overhauser effect data will aid in resolution. However, it should be emphasized that NMR usually provides essentially a kinetic assay of stability. Optical and calorimetric data are still desirable to provide a solid underpinning for NMR inferences. Even then, ambiguity is a problem: In Figure 3, for example, the kinetic data fit the extrapolated τ curve for the transition τ_4 nearly as well as for τ_1, and the agreement with τ_1 might appear fortuitous.

We were able to correlate the NMR rates with τ_1 only because in this case there was an equilibrium intensity loss that correlated with an optically inferred conformation change. NMR exchange measurements cannot really assay stability at high temperature where kinetics are rapid. Its main strength lies in the ability to see specific incipient changes at low temperature where the tRNA is intact and active. Spectroscopy of nonexchangeable nuclei is more useful at higher temperature.

An interesting study of tRNA thermal stability assayed by gentle chemical modification at moderate temperature was published by Rhodes (1977). Modification of bases by a carbodiimide reagent was assayed, by subsequent nuclease cleavage and two-dimensional chromatography, with and without Mg^{2+}. Since several hours were required for modification, the opening of the structure was not rate limiting as it is likely to be for most of our measurements. However, arguments were presented to indicate that the reagent was assaying structural mobility in the native conformation, rather than reagent-induced changes. The observations were not given directly in terms of rates, so what follows is to some extent an interpretation of Rhodes' paper.

In general, it appears that the variations in chemical reactivity are not as strongly dependent on temperature and Mg^{2+} concentration as are the NMR rates. Chemical reaction rates roughly doubled every 10 °C, and addition of Mg^{2+} required an increase in temperature of about 5 °C to achieve the same rate. The high-temperature NMR rates require very roughly half as big a change in temperature for the same rate change, and at least twice as big a change in temperature to compensate for Mg^{2+} concentration, compared to carbodiimide modification rates. On the other hand, the low-temperature NMR rates measured by the real-time method show temperature dependences about half as great as those of chemical modification rates.

The study by Rhodes lacks some of the uncertainties of our work which result from resonance assignment problems. Both methods indicate that GU4 is unstable, but there is not a clear indication of the simultaneous instability of AU pairs 5, 6, and 7 which we infer. In both bases, m^7G46 and G15–C48 appear unstable. The important tertiary interaction, G19–C56, is highly stable both with and without Mg^{2+}, according to Rhodes. We assign this base pair to the resonance of a proton whose stability is unusually Mg dependent although it is one of the most stable tertiary resonances in zero Mg^{2+} concentration. Likewise, we conclude that the U8–A14 interaction is highly Mg sensitive whereas according to chemical modification it appears less so. These differences could result from misassignment of NMR lines (especially for G19–C56) but may instead reflect the different nature of the two measurements.

It is of interest to compare our rate measurements with those of Mandal et al. (1979) on poly(rA-rU), obtained by stopped-flow spectrophotometry. Their estimate of the helix opening rate in zero $MgCl_2$ concentration falls on line B, Figure 9. It is reasonable that this rate would be a lower limit for tRNA secondary structure because helixes in tRNA are shorter than those studied by Mandal et al. (1979), and would be less stable. Their observations are consistent with our failure to observe real-time exchange at low temperatures in the absence of Mg^{2+}. The activation energy for real-time exchange of the most stable protons in unfractionated yeast tRNA (Johnston et al., 1979) in high magnesium concentration is somewhat less than the value of 17.6 kcal/mol for poly(rA-rU) found by Mandal et al. in zero magnesium concentration.

Recently, Ramstein & Buckingham (1980) have presented new tritium exchange data for tRNA. They find that several protons in unfractionated *E. coli* tRNA exchange in several hours and have also observed an interesting difference in exchange behavior between *E. coli* $tRNA^{Trp}$ and the UGA suppressor which differs in one base pair from it in the D stem. We have not been able to resolve such a large number of slowly exchanging downfield protons in our studies of various tRNA's, including unfractionated *E. coli* tRNA in high magnesium concentration (N. Figueroa, unpublished experiments), although we find that several downfield protons exchange in roughly 1 h. It is likely that the protons observed by Ramstein and Buckingham are amino protons; this interpretation is suggested by the work of Mandal et al. We previously reported

slow exchange for amino protons (Johnston et al., 1979), but a good quantitative estimate was difficult because of the large overlapping signal from aromatic carbon protons.

Our conclusions in zero $MgCl_2$ concentration for yeast $tRNA^{Phe}$ can be contrasted with those for *E. coli* $tRNA^{fMet}$ by Crothers and co-workers (Crothers et al., 1974; Stein & Crothers, 1976). In both cases, it is assumed that the tertiary structure unfolds, as seems reasonable and as is reported by the U8–A14 resonance. In the fMet species, the D stem was assumed to melt at more or less the same time as that of the tertiary structure, whereas we conclude in yeast $tRNA^{Phe}$ that the acceptor melts first. There is no obvious reason why the D stem should differ in stability between the two species, but the acceptor stem is expected to be highly stable for *E. coli* $tRNA^{fMet}$ since it contains six GC pairs. We cannot say with certainty that the D stem melts later than the acceptor because we lack sufficiently good NMR D-stem markers in yeast $tRNA^{Phe}$, and because we are studying kinetics rather than equilibria. It seems most reasonable that the D stem would be destabilized by tertiary melting as assumed by Crothers et al., but it also seems reasonable that the yeast $tRNA^{Phe}$ acceptor stem, terminating with three AU pairs, would likewise be destabilized.

Acknowledgments

We thank James Tropp, Valentina Sanchez, and Nara Figueroa for unpublished data and assistance and Dr. Brian Reid for the generous gift of *E. coli* $tRNA^{fMet}$.

References

Bolton, P. H., & Kearns, D. R. (1977) *Biochemistry 16*, 5729–5741.

Coutts, S. M., Riesner, D., Römer, R., Rabl, C. R., & Maas, G. (1975) *Biophys. Chem. 3*, 275–289.

Crothers, D. M. (1979) in *Transfer RNA: Structure, Properties, and Recognition* (Schimmel, P. R., Söll, D., & Abelson, J. N., Eds.) pp 163–176, Cold Spring Harbor Laboratory, Cold Spring Harbor, NY.

Crothers, D. M., & Cole, P. E. (1978) in *Transfer RNA* (Altman, S., Ed.) pp 196–247, MIT Press, Cambridge, MA.

Crothers, D. M., Cole, P. E., Hilbers, C. W., & Shulman, R. G. (1974) *J. Mol. Biol. 87*, 63–88.

Daniel, W. E., Jr., & Cohn, M. (1975) *Proc. Natl. Acad. Sci. U.S.A. 72*, 2582–2586.

Ehrenberg, M., Rigler, R., & Wintermeyer, W. (1979) *Biochemistry 18*, 4588–4599.

Englander, S. W., & Englander, J. J. (1978) *Methods Enzymol. 49*, 24–39.

Guéron, M., & Leroy, J. L. (1979) in *ESR and NMR of Paramagnetic Species in Biological and Related Systems* (Bertini, I., & Drago, R. S., Eds.) pp 327–367, Reidel, Dordrecht, The Netherlands.

Hilbers, C. W. (1979) in *Biological Applications of Magnetic Resonance* (Shulman, R. G., Ed.) pp 1–43, Academic Press, New York.

Hilbers, C. W., Robillard, G. T., Shulman, R. G., Blake, R. D., Webb, P. K., Fresco, R., & Riesner, D. (1976) *Biochemistry 15*, 1874–1882.

Hurd, R. E., & Reid, B. R. (1979) *Biochemistry 18*, 4017–4024.

Hurd, R. E., & Reid, B. R. (1980) *J. Mol. Biol. 142*, 181–194.

Johnston, P. D., & Redfield, A. G. (1977) *Nucleic Acids Res. 4*, 3599–3615.

Johnston, P. D., & Redfield, A. G. (1978) *Nucleic Acids Res. 5*, 3913–3927.

Johnston, P. D., & Redfield, A. G. (1979) in *Transfer RNA: Structure, Properties, and Recognition* (Abelson, J., Schimmel, P. R., & Söll, D., Eds.) pp 191–206, Cold Spring Harbor Laboratory, Cold Spring Harbor, NY.

Johnston, P. D., & Redfield, A. G. (1981) *Biochemistry 20*, 1147–1156.

Johnston, P. D., Figueroa, N., & Redfield, A. G. (1979) *Proc. Natl. Acad. Sci. U.S.A. 76*, 3130–3134.

Kearns, D. R., & Bolton, P. H. (1978) in *Biomolecular Structure and Function* (Agris, P. F., Ed.) pp 493–516, Academic Press, New York.

Kim, S.-H. (1978) in *Transfer RNA* (Altman, S., Ed.) pp 248–293, MIT Press, Cambridge, MA.

Lightfoot, D. R., Wong, K. L., Kearns, D. R., & Reid, B. R. (1973) *J. Mol. Biol. 78*, 71–89.

Mandal, C., Kallenbach, N. R., & Englander, S. W. (1979) *J. Mol. Biol. 135*, 391–411.

Privalov, P. L., & Filimonov, V. V. (1978) *J. Mol. Biol. 122*, 447–464.

Ramstein, J., & Buckingham, R. H. (1980) *Proc. Natl. Acad. Sci. U.S.A. 78*, 1567–1571.

Reid, B. R., Ribeiro, N. S., McCollum, L., Abbate, J., & Hurd, R. E. (1977) *Biochemistry 16*, 2086–2094.

Rhodes, D. (1977) *Eur. J. Biochem. 81*, 91–101.

Robillard, G. T., & Reid, B. R. (1979) in *Biological Applications of Magnetic Resonance* (Shulman, R. G., Ed.) p 45, Academic Press, New York.

Romaniuk, P. J., Hughes, D. W., Gregoire, R. J., Bell, R. A., & Neilson, T. (1979) *Biochemistry 18*, 5109–5116.

Römer, R., & Varadi, V. (1977) *Proc. Natl. Acad. Sci. U.S.A. 74*, 1561–1564.

Sanchez, V., Redfield, A. G., Johnston, P., & Tropp, J. S. (1980) *Proc. Natl. Acad. Sci. U.S.A. 77*, 5659–5662.

Schimmel, P. R., & Redfield, A. G. (1980) *Annu. Rev. Biophys. Bioeng. 9*, 181–222.

Stein, A., & Crothers, D. M. (1976) *Biochemistry 15*, 160–168.

Urbanke, C., Römer, R., & Maass, G. (1975) *Eur. J. Biochem. 55*, 439–444.

Wong, K. L., Wong, Y. P., & Kearns, D. R. (1975) *Biopolymers 14*, 749–762.